RM E55L13a

NACA

RESEARCH MEMORANDUM

DYNAMICS OF A SUPERSONIC INLET WITH ADJUSTABLE BYPASS IN COMBINATION WITH A J34 TURBOJET ENGINE

By Fred Wilcox and Paul Whalen

Lewis Flight Propulsion Laboratory
Cleveland, Ohio

NATIONAL ADVISORY COMMITTEE FOR AERONAUTICS

WASHINGTON

March 23, 1956
Declassified February 10, 1959

NATIONAL ADVISORY COMMITTEE FOR AERONAUTICS

RESEARCH MEMORANDUM

DYNAMICS OF A SUPERSONIC INLET WITH ADJUSTABLE BYPASS IN COMBINATION WITH A J34 TURBOJET ENGINE

By Fred Wilcox and Paul Whalen

SUMMARY

The dynamics of an axially symmetric supersonic inlet with an adjustable bypass in combination with a J34 turbojet engine were investigated at free-stream Mach numbers of 1.8 and 2.0 in the Lewis 8- by 6-foot supersonic tunnel. The transient response of a normal-shock-sensing system for the shock located near the sensing orifice and the transient response of the compressor-inlet total pressure to bypass-door-position disturbances were obtained. Within the accuracy of the data, it appears that these transient responses may be reasonably predicted from steady-state inlet and engine performance data.

INTRODUCTION

In order to obtain optimum turbojet engine performance over a range of supersonic flight speeds and ambient temperatures, variable-geometry features are required in the inlet. The bypass has been shown to be an efficient device for matching the inlet to the engine (ref. 1), and the use of shock-positioning control systems for regulation of the bypass has been demonstrated (refs. 2 and 3). A knowledge of the dynamics of the inlet is necessary (ref. 4) in order to describe more completely the operation of these inlet control systems and to determine interaction effects between inlet and engine control systems.

The dynamics of a spike-type axially symmetric inlet were investigated in the NACA Lewis 8- by 6-foot supersonic tunnel at Mach numbers of 1.8 and 2.0 for the engine-inlet combination reported in references 3 and 5. The response of a normal-shock sensor of the type employed in reference 3 to sinusoidal bypass-door-position changes was obtained for normal-shock location near the shock-sensing orifice. In addition, the response of the compressor-inlet total pressure to ramp changes in bypass-door position was obtained at constant engine fuel flow. Also included is a derivation (appendix A) by John C. Sanders of the Lewis laboratory for the response of the compressor-inlet total pressure to small changes in bypass flow area.

SYMBOLS

The following symbols are used in this report:

A	flow area, sq ft
$A_{b,max}$	maximum bypass flow area, 0.2695 sq ft
A_f	compressor rotor frontal area, 1.98 sq ft
M	Mach number
N	engine speed, rpm
N^*	rated engine speed, 12,500 rpm
$\frac{N}{N^*\sqrt{\theta}}$	corrected engine-speed parameter
P	total pressure, lb/sq ft
ΔP	pressure change, lb/sq ft
p	static pressure, lb/sq ft
$\frac{p_p - p_c}{p_0}$	static-pressure parameter
r	rise ratio, $\Delta P_i/\Delta P_{eq}$
s	Laplace variable
w_a	air flow, lb/sec
$\frac{w_a\sqrt{\theta}}{\delta A_f}$	corrected air-flow parameter, lb/(sec)(sq ft)
w_f	fuel flow, lb/sec
$\frac{w_f}{\delta\sqrt{\theta}}$	corrected fuel-flow parameter, lb/sec
δ	total pressure at station 3 divided by NACA standard sea-level static pressure

θ stream total temperature divided by NACA standard sea-level static temperature

θ_l angle between axis of spike and line joining cone apex and cowl lip, deg

τ_i time constant of engine evaluated at constant total pressure at compressor inlet

Subscripts:

b bypass

c cone surface

eq equilibrium

i instantaneous conditions at conclusion of a change in bypass-door position

p probe on cowl lip

0 free stream

2 in diffuser ahead of bypass

3 compressor inlet

APPARATUS

A sketch of the nacelle showing the engine-inlet installation and the dynamic instrumentation is given in figure 1.

Engine-inlet combination. - The J34 engine-inlet combination used in this investigation is described in reference 5. The translating cone of the inlet was set so that the angle θ_l was 42.0° at Mach number 2.0 and 45.0° at Mach number 1.8. At these settings the oblique shock fell approximately 3/8 inch ahead of the cowl lip. Bypass air was bled through a series of longitudinal slots in the outer wall of the subsonic diffuser to a cavity between the diffuser wall and the nacelle skin and then discharged to the free stream through the bypass door.

Bypass-door hydraulic servoactuator. - The bypass air flow was varied by the use of a hinged door mounted in the nacelle skin and actuated by a hydraulic servo. In response to position error voltage (fig. 1), a pilot valve metered high-pressure oil to the actuating cylinder.

The change in bypass-door position was the time integral of the error voltage signal. In order to study the inlet dynamics, provision was made to apply step and sinusoidal input voltages to the servomechanism. The response of the bypass door to constant-amplitude sinusoidal input voltages is shown in figure 2. The amplitude ratio, defined as the ratio of bypass-door oscillation to the amplitude at 1 cycle per second, decreased to a value of approximately 0.08 at 22 cycles per second. The bypass-door movement lagged the input voltage signal by about 110° at 22 cycles per second. The bypass door required a minimum of 0.2 second to fully open or close when a step change in input voltage was applied.

Normal-shock sensor. - The normal-shock sensing installation on this model consisted of a pressure transducer connected between a static-pressure probe extending from the cowl lip and a static-pressure tap on the inlet cone. The output of the transducer indicated whether the inlet normal shock was ahead of or behind the cowl-lip probe. This sensing system was a part of the shock-positioning control reported in reference 3.

INSTRUMENTATION

Recorder. - All transient data were recorded on a multichannel recording oscillograph. The oscillograph apparatus had an effective time constant of less than 0.005 second.

Bypass-door position. - The piston of the hydraulic servo was mechanically attached to the moving contact of a slide-wire potentiometer and the voltage calibrated in terms of door position. The response of this system was limited only by the mechanical response of the servosystem.

Pressures. - Pressure transients were measured with bridge-type strain-gage pressure pickups energized by a 3000-cycle carrier system. The apparent time constant of the pressure pickups was 0.3 millisecond. Steady-state pressures were recorded by an automatic digital pressure recorder.

PROCEDURE

Disturbances were imposed on the engine-inlet system by changes in bypass-door position at constant engine fuel flow. Inlet dynamics were obtained by recording the response of the normal-shock sensor and the compressor-inlet total pressure to these disturbances. Sinusoidal variations in bypass-door position were obtained by applying a sinusoidal input voltage to the servosystem. Ramp-type variations in bypass-door position were the result of applying step changes in input voltage.

RESULTS AND DISCUSSION

The effects of bypass-door-position disturbances on the normal-shock sensor output and on the compressor-inlet total pressure were greatly different. Accordingly, these effects will be treated separately.

Normal-Shock Sensor

The steady-state variation of a static-pressure parameter with corrected inlet air flow is presented in figure 3 for free-stream Mach numbers of 1.8 and 2.0. The parameter presented is the difference between the cowl-lip-probe pressure and the cone reference pressure divided by the free-stream static pressure. The sensor output is proportional to the pressure differential.

The data indicate that as the corrected inlet air flow is decreased and the normal shock moves ahead of the cowl-lip probe an abrupt rise in sensor output results. Because of the small change in inlet air flow required to pass the normal shock across the probe, a large change in sensor output is obtained for a small movement of the bypass door when the shock is initially in the region of the probe.

Values of static-pressure parameter calculated from theoretical local static pressures are included for comparison. The differences between measured and calculated values are presumably due to three-dimensional effects and misalinement of the probe with the local flow direction. The dip in the Mach number 2.0 data over the unsteady flow region, however, is due to an averaging by the steady-state pressure recording system of high and low pressures as the normal shock oscillates over the cowl-lip probe.

With the normal shock initially in equilibrium very near the sensing orifice, data were taken at Mach number 2.0 with sinusoidal variations in bypass-door position of sufficient amplitude to pass the normal shock across the sensing orifice. The frequency of the oscillation was varied from 1 to 22 cycles per second while the amplitude was held constant. A typical trace showing the response of the normal-shock sensor for a bypass-door oscillation frequency of 9 cycles per second is shown in figure 4. The sensor response is a rather irregular rectangular wave of large amplitude going between differential static-pressure ratios of 0.1 and 2.2. These values are in agreement with the data of figure 3. The response of the shock sensor lags the bypass-door movement.

The amplitude ratio and phase lag calculated from traces such as figure 4 are presented in figure 5 for frequencies from 1 to 22 cycles per second. The amplitude ratio is defined as the amplitude of the shock-sensor fluctuation divided by the amplitude of fluctuation at a frequency

of 1 cycle per second. The fact that the amplitude ratio was nearly 1 for frequencies up to the maximum of 22 cycles per second indicated that the normal shock was moving across the sensing orifice.

Phase lag increased linearly from a value of nearly zero at the lowest frequency to over 100° at the highest frequency. This linear variation in phase lag suggests that a constant time delay existed between movement of the bypass door and the response of the normal-shock sensor. It is believed that this delay was the time required for a sound wave to move upstream from the bypass exit to the shock. A delay time computed by the methods of reference 6 with the assumption that a sound wave was propagated along the shortest possible path resulted in a time delay of 0.0104 second. The data of figure 5 indicate that this number is low. Because the air discharged by the bypass came from a cavity surrounding the diffuser wall, the average path was longer. Accordingly, another calculation was made to include the time required for a sound wave to travel half the distance around the annular cavity surrounding the diffuser (fig. 1). For this calculation, the delay time was increased to 0.0125 second, which is generally in good agreement with the data.

The response of the normal-shock sensor to a step change in bypass-door position with the normal shock initially just downstream of the sensing orifice is inferred from figure 5 and shown in the following sketch:

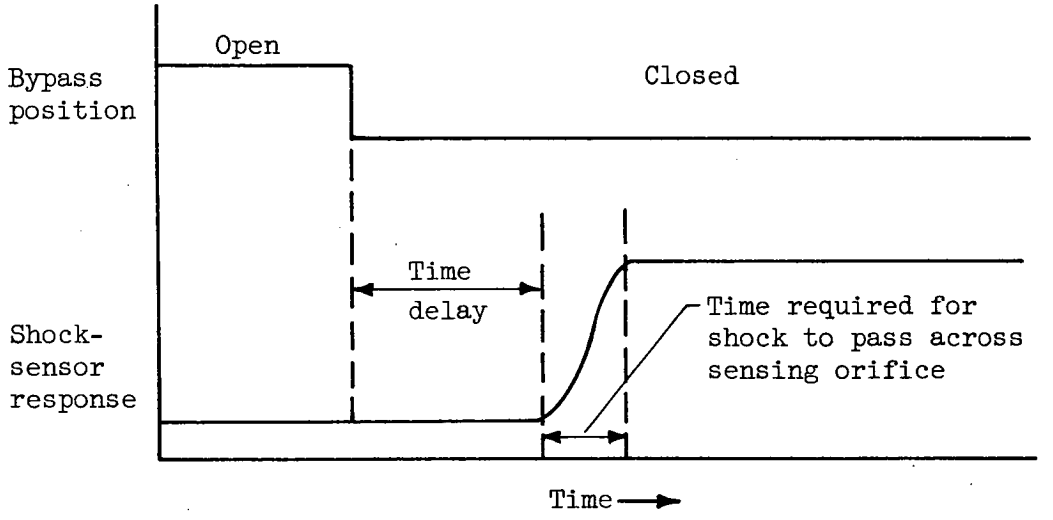

If the bypass door is instantaneously closed, the normal shock begins to move after the delay time. Some finite time is required for the sensor pressure to reach its final value. Factors affecting this time are the rate of change of the sensor pressure with corrected air flow (fig. 3) and the rate of change of corrected air flow. For these tests where the

rate of travel of the bypass door limited the rate of change of corrected air flow, the time required for the sensor pressure to reach its final value was about 0.008 second.

When the normal shock is initially some distance from the shock-sensing orifice, a greater time delay exists. This additional time is the time required for the normal shock to move to the sensing orifice. The evaluation of this time interval is beyond the scope of this discussion.

Compressor-Inlet Pressure

A representative trace of the dynamic response of the compressor-inlet total pressure to a change in bypass-door position with the engine fuel flow maintained constant is shown in figure 6. In this example the inlet operation was initially supercritical. Increasing the bypass area from 36 to 87 percent of maximum caused the inlet operation to become further supercritical and dropped the diffuser pressure recovery from 0.89 to 0.83. Indicated on the figure are the initial pressure change ΔP_i, measured at the conclusion of bypass-door travel, and the final pressure change ΔP_{eq}, measured at equilibrium.

If a turbojet engine is considered as a linear system, the compressor-inlet pressure response ΔP_3 at any instant to an imposed bypass-area disturbance ΔA_b at constant actual fuel flow is of the form

$$\Delta P_3 = \frac{\left[1 + r\left(\frac{\tau_i}{r}\right)s\right]}{\left[1 + \left(\frac{\tau_i}{r}\right)s\right]} \left.\frac{\partial P}{\partial A_b}\right|_{W_f} \Delta A_b \qquad (1)$$

This equation is derived in appendix A. The response predicted by equation (1) is presented in the following sketch for a step change in bypass-door position at supercritical inlet operation and constant engine fuel flow:

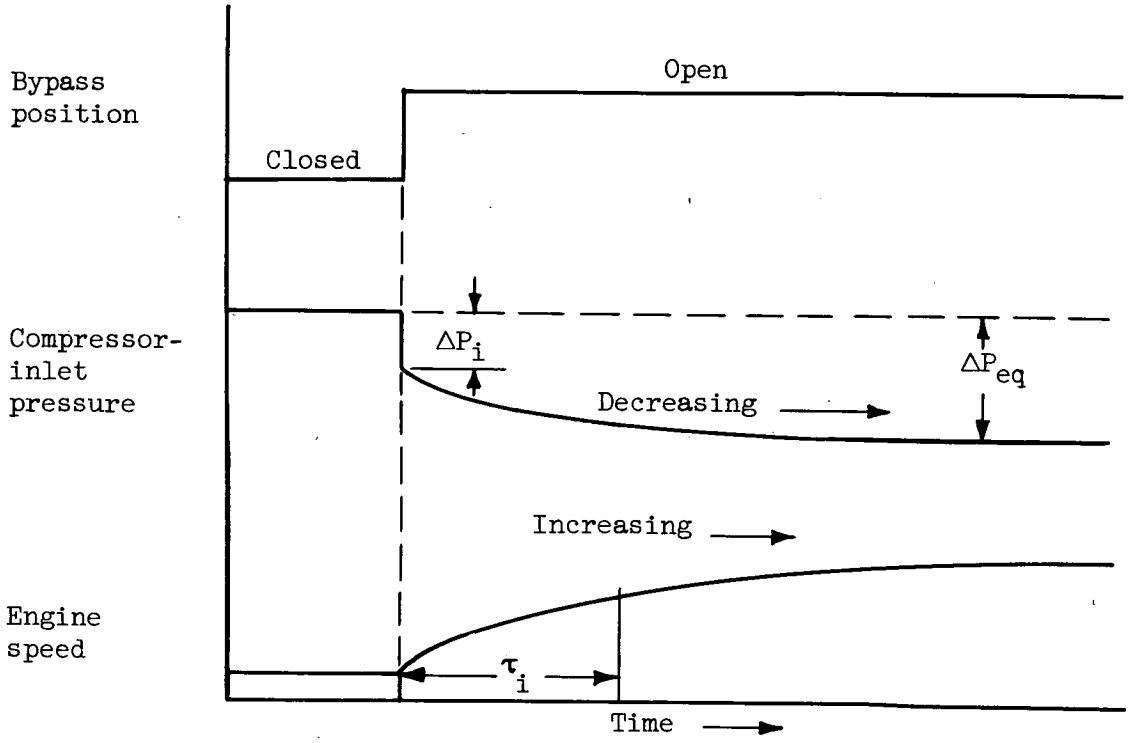

The parameters of the compressor-inlet pressure response, ΔP_i and ΔP_{eq}, may be calculated with a fair degree of accuracy for any initial operating conditions and bypass-door position change from steady-state engine-inlet performance. These quantities, with the engine time constant and equation (1), define the compressor-inlet transient pressure response to a change in bypass-door position at a constant engine fuel flow.

Calculation of rise ratio from steady-state engine-inlet performance. - The steady-state inlet performance for this test is shown in figures 7 and 8. In figure 7, the diffuser total-pressure recovery P_3/P_0 is given as a function of corrected inlet air flow based on the frontal area of the compressor rotor (1.98 sq ft) and the diffuser pressure. Inlet air flow is defined as the total air flow ahead of the bypass. In figure 8, maximum corrected bypass air flow for the bypass door fully open is given as a function of diffuser pressure recovery. A flow coefficient of 1 was assumed in computing the bypass air flow for the bypass door partly open. Corrected engine air flow is the difference between inlet and bypass corrected air flows.

The steady-state performance curves of the test engine are given in figure 9. Corrected engine air flow and corrected fuel flow are shown as functions of corrected engine speed based on the rated speed of 12,500 rpm.

For small changes in bypass flow area when the diffuser and engine parameters are essentially linear, the parameters r and $\left.\frac{\partial P_3}{\partial A_b}\right|_{W_f}$ of equation (1) may be evaluated from steady-state engine-inlet performance by the methods of appendix A. For the runs made in this test, the changes in bypass flow area were large and the range of operation often extended into nonlinear regions of the diffuser performance curves. In these cases the rise ratio $\Delta P_i/\Delta P_{eq}$ and the final amplitude $\Delta P_{eq} = \left.\frac{\partial P_3}{\partial A_b}\right|_{W_f} \Delta A_b$ were determined by assuming a quasi-steady-state process and by working directly with the engine and inlet performance curves. The change in corrected bypass air flow is found from figure 8. Because the engine cannot change speed instantaneously, the change in corrected bypass air flow produces an equal change in corrected inlet air flow and therefore a change in diffuser pressure recovery (fig. 7). This instantaneous change is ΔP_i.

Because of the change in diffuser pressure recovery, the value of corrected fuel flow changes for a constant fuel-flow rate. This change in corrected fuel flow requires that the engine change speed and, therefore, the corrected engine air-flow requirements change. If the bypass door is held in its new position, the change in corrected engine air flow produces an equal change in corrected inlet air flow and, therefore, a change in diffuser pressure recovery. These changes imply a further change in corrected fuel flow, and the computation cycle repeats, converging rapidly, however, to the equilibrium operating conditions for the engine-inlet combination. The pressure recovery at this operating point defines the total change in pressure ΔP_{eq}. An example is included in appendix B in order to illustrate this calculation.

A comparison of rise ratios calculated by this method with those measured experimentally by imposing ramp changes in bypass-door position (see fig. 6) is presented in table I. The initial and final steady-state operating conditions of the engine and inlet are also presented. The agreement between measured and calculated values of rise ratio is reasonably good, in most cases being within the accuracy of the measured values. Calculations indicate that the use of a ramp change rather than a step change in bypass-door position introduces less than 10 percent error in the measured rise ratio.

For some of the runs of table I, rise ratios greater than 1 were obtained. Values greater than 1 result when changes in engine speed due to the bypass step cause a change in diffuser pressure recovery which is in opposition to the change resulting from the bypass. Runs 6 and 10 of table I are examples in which the initial and final inlet operating

points are on the opposite side of the peak diffuser pressure recovery. Runs 7 and 8 are examples of an engine speed change causing a change in diffuser corrected air flow opposite to that of the bypass. For run 7, the inlet operating point was taken from subcritical to nearly critical by the bypass step with an increase in pressure recovery. The resulting decrease in engine speed lowered the pressure recovery by causing operation in the subcritical region. The bypass step of run 8 lowered diffuser pressure recovery by taking inlet operation from a slightly subcritical operating condition to further subcritical operation. The resulting increase in engine speed raised pressure recovery by increasing inlet air flow.

SUMMARY OF RESULTS

From an investigation of the response of a normal-shock-sensing system and of the compressor-inlet total pressure to bypass-door-position disturbances at constant engine fuel flow, the following results were obtained:

1. Within the accuracy of the data, the compressor-inlet pressure response to a change in bypass-door position is defined by a rise ratio and the engine time constant. The rise ratio may be computed approximately from steady-state engine-inlet performance.

2. The response of a normal-shock sensor located on the cowl-lip probe indicated that a minimum time delay existed. The calculated value of this minimum delay time agreed with experimental data.

Lewis Flight Propulsion Laboratory
National Advisory Committee for Aeronautics
Cleveland, Ohio, December 13, 1955

APPENDIX A

COMPRESSOR-INLET PRESSURE RESPONSE

By John C. Sanders

If certain functional relations among the diffuser and engine variables are assumed, the dynamic behavior of the compressor-inlet total pressure can be described by a first-order transfer function that agrees with experimental data. This transfer function is restricted by the following assumptions:

(1) Linearization about an arbitrary operating point applies.

(2) Conditions of flight speed and altitude are constant.

(3) All thermodynamic and flow processes are quasi-static.

(4) The only major storage element is the engine rotor inertia.

For small excursions from an arbitrary operating point assume that

$$P_3 = K\left(\frac{W_{a,3}}{\delta} + \frac{W_{a,b}}{\delta}\right)$$

Then

$$\Delta P_3 = K\Delta\left(\frac{W_{a,3}}{\delta}\right) + K\Delta\left(\frac{W_{a,b}}{\delta}\right) \tag{A1}$$

The term $\Delta\left(\frac{W_{a,3}}{\delta}\right)$ may be expressed in terms of the engine variables

$$\Delta\left(\frac{W_{a,3}}{\delta}\right) = \left.\frac{\partial\left(\frac{W_{a,3}}{\delta}\right)}{\partial N}\right|_{P_3} \Delta N + \left.\frac{\partial\left(\frac{W_{a,3}}{\delta}\right)}{\partial P_3}\right|_{N} \Delta P_3$$

and $\Delta\left(\frac{W_{a,b}}{\delta}\right)$ may be expressed in terms of the bypass flow area and the compressor-inlet pressure

$$\Delta\left(\frac{W_{a,b}}{\delta}\right) = \left.\frac{\partial\left(\frac{W_{a,b}}{\delta}\right)}{\partial P_3}\right|_{A_b} \Delta P_3 + \left.\frac{\partial\left(\frac{W_{a,b}}{\delta}\right)}{\partial A_b}\right|_{P_3} \Delta A_b$$

The change in engine speed at constant fuel flow may be expressed as

$$\Delta N = \frac{\left.\frac{\partial N}{\partial P_3}\right|_{W_f}}{\tau_i s + 1} \Delta P_3$$

Rewriting equation (A1) with the expansions indicated yields

$$\Delta P_3 = K\left.\frac{\partial\left(\frac{W_{a,b}}{\delta}\right)}{\partial P_3}\right|_{A_b} \Delta P_3 + K\left.\frac{\partial\left(\frac{W_{a,b}}{\delta}\right)}{\partial A_b}\right|_{P_3} \Delta A_b + K\left.\frac{\partial\left(\frac{W_{a,3}}{\delta}\right)}{\partial P_3}\right|_{N} \Delta P_3 + K\left.\frac{\partial\left(\frac{W_{a,3}}{\delta}\right)}{\partial N}\right|_{P_3} \frac{\left.\frac{\partial N}{\partial P_3}\right|_{W_f}}{\tau_i s + 1} \Delta P_3$$

Solving for ΔP_3 gives

$$\Delta P_3 = \frac{K\left.\frac{\partial\left(\frac{W_{a,b}}{\delta}\right)}{\partial A_b}\right|_{P_3}}{1 - K\left.\frac{\partial\left(\frac{W_{a,3}}{\delta}\right)}{\partial P_3}\right|_{N} - K\left.\frac{\partial\left(\frac{W_{a,b}}{\delta}\right)}{\partial P_3}\right|_{A_b} - K\left.\frac{\partial\left(\frac{W_{a,3}}{\delta}\right)}{\partial N}\right|_{P_3}\left.\frac{\partial N}{\partial P_3}\right|_{W_f}} \frac{(\tau_i s + 1)\Delta A_b}{\frac{\tau_i}{1 - \frac{K\left.\frac{\partial\left(\frac{W_{a,3}}{\delta}\right)}{\partial N}\right|_{P_3}\left.\frac{\partial N}{\partial P}\right|_{W_f}}{1 - K\left.\frac{\partial\left(\frac{W_{a,3}}{\delta}\right)}{\partial P_3}\right|_{N} - K\left.\frac{\partial\left(\frac{W_{a,b}}{\delta}\right)}{\partial P_3}\right|_{A_b}}} s + 1}$$

which has the form

$$\Delta P_3 = \frac{\left[1 + r\left(\frac{\tau_i}{r}\right)s\right]}{\left[1 + \left(\frac{\tau_i}{r}\right)s\right]} \left.\frac{\partial P}{\partial A_b}\right|_{W_f} \Delta A_b \qquad (1)$$

where the rise ratio r is

$$r = 1 - \frac{\left.\frac{\partial\left(\frac{w_{a,3}}{\delta}\right)}{\partial N}\right|_{P_3} \left.\frac{\partial N}{\partial P_3}\right|_{w_f}}{\frac{1}{K} - \left.\frac{\partial\left(\frac{w_{a,3}}{\delta}\right)}{\partial P_3}\right|_{N} - \left.\frac{\partial\left(\frac{w_{a,b}}{\delta}\right)}{\partial P_3}\right|_{A_b}}$$

and

$$\left.\frac{\partial P_3}{\partial A_b}\right|_{w_f} = \frac{\left.\frac{\partial\left(\frac{w_{a,b}}{\delta}\right)}{\partial A_b}\right|_{P_3}}{\frac{1}{K} - \left.\frac{\partial\left(\frac{w_{a,3}}{\delta}\right)}{\partial P_3}\right|_{N} - \left.\frac{\partial\left(\frac{w_{a,b}}{\delta}\right)}{\partial P_3}\right|_{A_b} - \left.\frac{\partial\left(\frac{w_{a,3}}{\delta}\right)}{\partial N}\right|_{P_3} \left.\frac{\partial N}{\partial P_3}\right|_{w_f}}$$

APPENDIX B

EXAMPLE OF CALCULATION OF RISE RATIO BY ITERATION METHOD

Following is a numerical calculation of run 5, table I.

(1) The steady-state conditions before the bypass-door movement are

Corrected engine speed $\frac{N}{N^*\sqrt{\theta}} = 0.806$

Bypass area ratio $\frac{A_b}{A_{b,max}} = 0.36$

Corrected fuel flow $\frac{w_f}{\delta\sqrt{\theta}} = 0.292$ lb/sec

Corrected engine air flow $\frac{w_{a,3}\sqrt{\theta}}{\delta A_f} = 23.30$ lb/(sec)(sq ft)

Corrected bypass air flow $\frac{w_{a,b}\sqrt{\theta}}{\delta A_f} = 2.08$ lb/(sec)(sq ft)

Corrected inlet air flow $\frac{w_{a,2}\sqrt{\theta}}{\delta A_f} = 25.38$ lb/(sec)(sq ft)

Pressure recovery $\frac{P_3}{P_0} = 0.889$

(2) When the bypass door is instantaneously opened to $\frac{A_b}{A_{b,max}} = 0.87$, the engine speed and corrected engine air flow are momentarily constant. If a quasi-steady state is assumed,

Corrected engine air flow $\left(\frac{w_{a,3}\sqrt{\theta}}{\delta A_f}\right)_i = 23.30$ lb/(sec)(sq ft)

Corrected bypass air flow $\left.\frac{w_{a,b}\sqrt{\theta}}{\delta A_f}\right|_N = 4.95$ lb/(sec)(sq ft)

Corrected inlet air flow $\left.\frac{w_{a,2}\sqrt{\theta}}{\delta A_f}\right|_N = 28.25$ lb/(sec)(sq ft)

Pressure recovery $\left(\frac{P_3}{P_0}\right)_i = 0.845$

(3) Since the actual fuel flow is held constant, the change in pressure recovery which has occurred following the opening of the bypass door increases the value of corrected fuel flow $\frac{w_f}{\delta\sqrt{\theta}}$ to 0.307 pound per second. The engine accelerates towards the steady-state condition set by this value of corrected fuel flow, and the new operating conditions are

Corrected engine speed $\frac{N}{N^*\sqrt{\theta}} = 0.815$

Corrected engine air flow $\frac{w_{a,3}\sqrt{\theta}}{\delta A_f} = 23.70$ lb/(sec)(sq ft)

Corrected bypass air flow $\frac{w_{a,b}\sqrt{\theta}}{\delta A_f} = 4.93$ lb/(sec)(sq ft)

Corrected inlet air flow $\frac{w_{a,2}\sqrt{\theta}}{\delta A_f} = 28.63$ lb/(sec)(sq ft)

Pressure recovery $\frac{P_3}{P_0} = 0.834$

(4) As the pressure recovery at this steady state differs from that at the previous state, the value of corrected fuel flow assumes a new value; $\frac{w_f}{\delta\sqrt{\theta}} = 0.311$ pound per second. The operating conditions continue to change and ultimately approach an equilibrium condition.

Corrected engine speed $\frac{N}{N^*\sqrt{\theta}} = 0.818$

Corrected engine air flow $\frac{w_{a,3}\sqrt{\theta}}{\delta A_f} = 23.80$ lb/(sec)(sq ft)

Corrected bypass air flow $\frac{w_{a,b}\sqrt{\theta}}{\delta A_f} = 4.93$ lb/(sec)(sq ft)

Corrected inlet air flow $\frac{w_{a,2}\sqrt{\theta}}{\delta A_f} = 28.73$ lb/(sec)(sq ft)

Pressure recovery $\frac{P_3}{P_0} = 0.831$

The rise ratio computed from these values is

$$\frac{\Delta P_i}{\Delta P_{eq}} = \frac{\left.\frac{P_3}{P_0}\right|_{initial} - \left.\frac{P_3}{P_0}\right|_{i}}{\left.\frac{P_3}{P_0}\right|_{initial} - \left.\frac{P_3}{P_0}\right|_{eq}} = \frac{0.889 - 0.845}{0.889 - 0.831} = 0.76$$

The measured rise ratio is

$$\frac{\Delta P_i}{\Delta P_{eq}} = 0.65$$

For comparison, the measured pressure recovery at equilibrium was 0.828, as compared with the computed value of 0.831.

REFERENCES

1. Allen, J. L., and Beke, Andrew: Performance Comparison at Supersonic Speeds of Inlet Spilling Excess Mass Flow by Means of Bow Shock, Conical Shock, and Bypass. NACA RM E53H11, 1953.

2. Leissler, L. Abbott, and Nettles, J. Cary: Investigation to Mach Number 2.0 of Shock-Positioning Control Systems for a Variable-Geometry Inlet in Combination with a J34 Turbojet Engine. NACA RM E54I27, 1954.

3. Wilcox, F. A.: Investigation of a Continuous Normal-Shock Positioning Control on the Bypass of a Supersonic Inlet in Combination with the J34 Turbojet Engine. NACA RM E55J10, 1956.

4. Pack, George J., and Phillips, W. E., Jr.: Analog Study of Interacting and Noninteracting Multiple-Loop Control Systems for Turbojet Engines. NACA TN 3112, 1954.

5. Nettles, J. C., and Leissler, L. A.: Investigation of Adjustable Supersonic Inlet in Combination with J34 Engine up to Mach 2.0. NACA RM E54H11, 1954.

6. Wilcox, Fred A., and Anderson, Arthur R.: An Analysis of Ram-Jet Engine Time Delay Following a Fuel-Flow Disturbance. NACA RM E55D22, 1955.

7. Delio, Gene J., and Rosenzweig, Solomon: Dynamic Response at Altitude of a Turbojet Engine with Variable Area Exhaust Nozzle. NACA RM E51K19, 1952.

TABLE I. - COMPARISON OF MEASURED AND CALCULATED RISE RATIOS

Run	Mach number, M_0	Initial conditions measured			Bypass step	Equilibrium conditions				Rise ratio, $\frac{\Delta P_i}{\Delta P_{eq}}$	
						Measured		Calculated			
		Bypass area, $\frac{A_b}{A_{b,max}}$	Corrected engine speed, $\frac{N}{N^*\sqrt{\theta}}$	Diffuser total-pressure recovery, $\frac{P_3}{P_0}$	Bypass area, $\frac{A_b}{A_{b,max}}$	Corrected engine speed, $\frac{N}{N^*\sqrt{\theta}}$	Diffuser total-pressure recovery, $\frac{P_3}{P_0}$	Corrected engine speed, $\frac{N}{N^*\sqrt{\theta}}$	Diffuser total-pressure recovery, $\frac{P_3}{P_0}$	Measured	Calculated
1	2.0	0.0	0.865	0.894	1.00	0.901	0.732	0.900	0.732	0.65	0.83
2		1.00	.901	.732	.0	.865	.894	.865	.894	.95	.89
3		.0	.878	.892	1.00	.919	.719	.918	.720	.70	.84
4		1.00	.919	.719	.0	.878	.892	.878	.894	.85	.78
5 (fig. 6)		.36	.806	.889	.87	.821	.828	.817	.831	.65	.76
6		.87	.821	.828	.36	.806	.889	.808	.890	1.00	1.06
7	1.8	0.0	0.800	0.879	1.00	0.796	0.925	0.791	0.925	1.10	1.02
8		1.00	.796	.925	.0	.800	.879	.800	.879	1.10	1.02
9		.0	.927	.922	.71	.946	.849	.943	.850	.70	.81
10		.71	.946	.849	.0	.927	.922	.929	.924	1.10	1.03

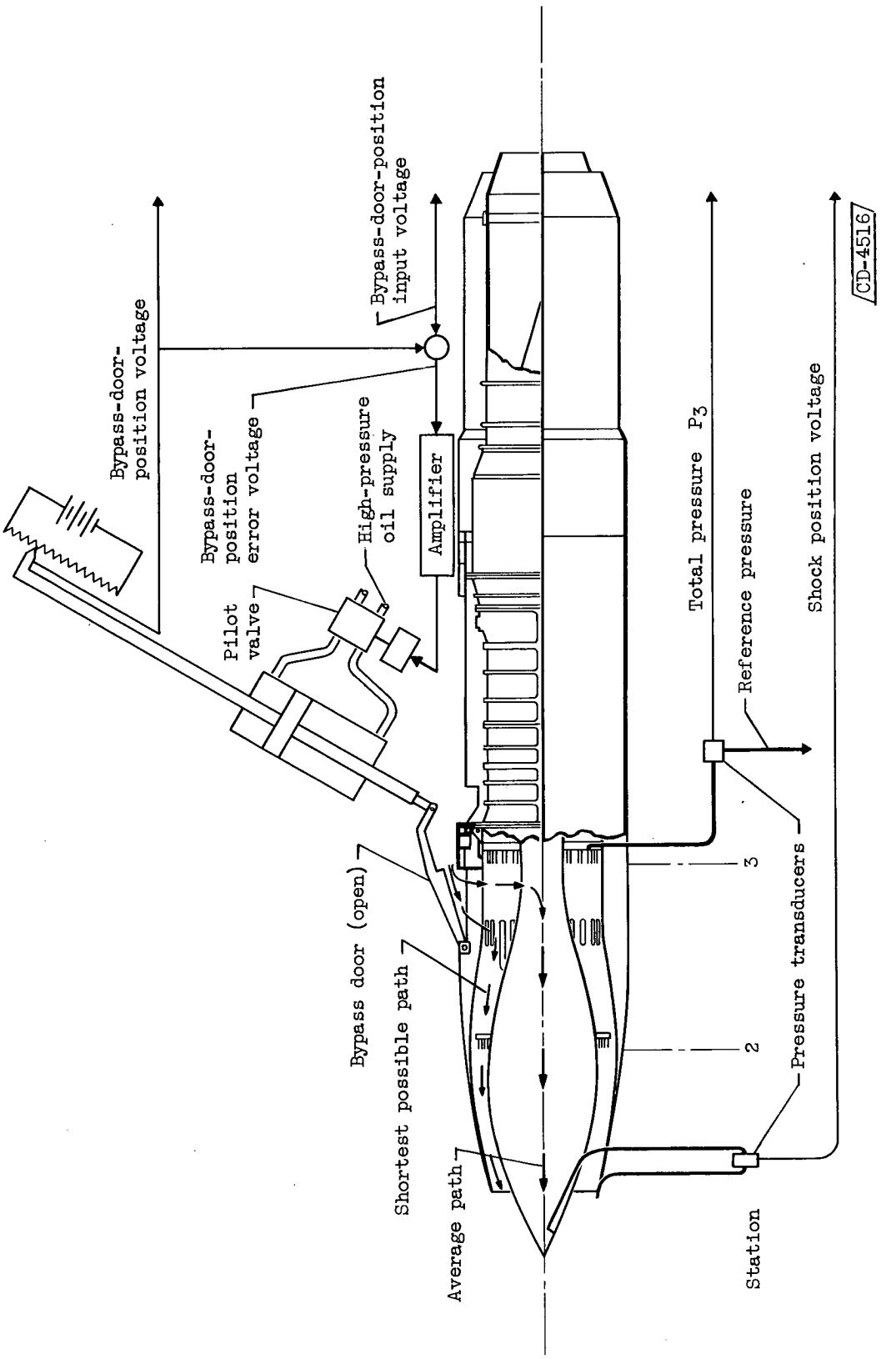

Figure 1. - Schematic diagram of J34 turbojet engine-inlet installation.

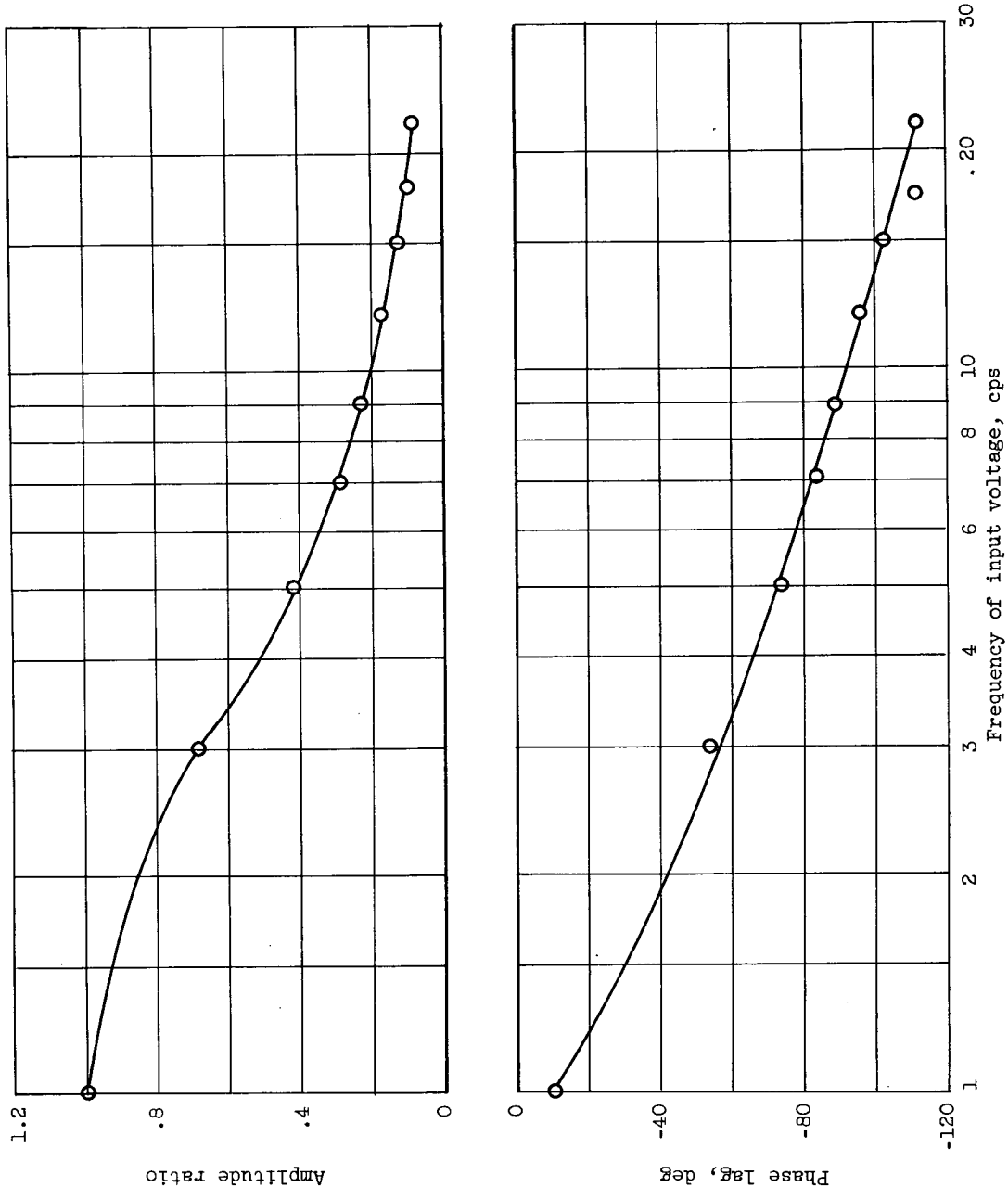

Figure 2. - Dynamic response of bypass door.

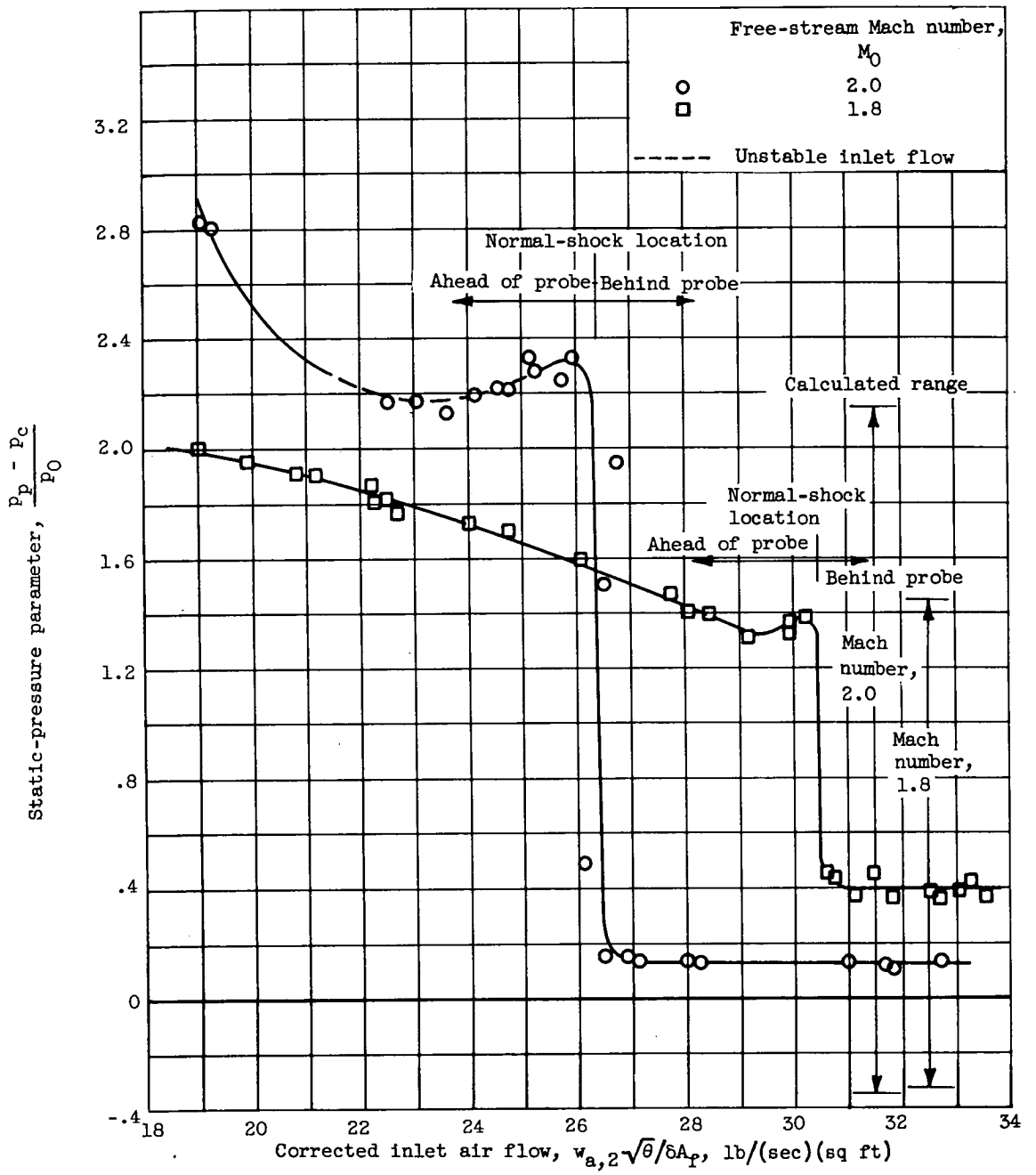

Figure 3. - Steady-state variation of static-pressure parameter.

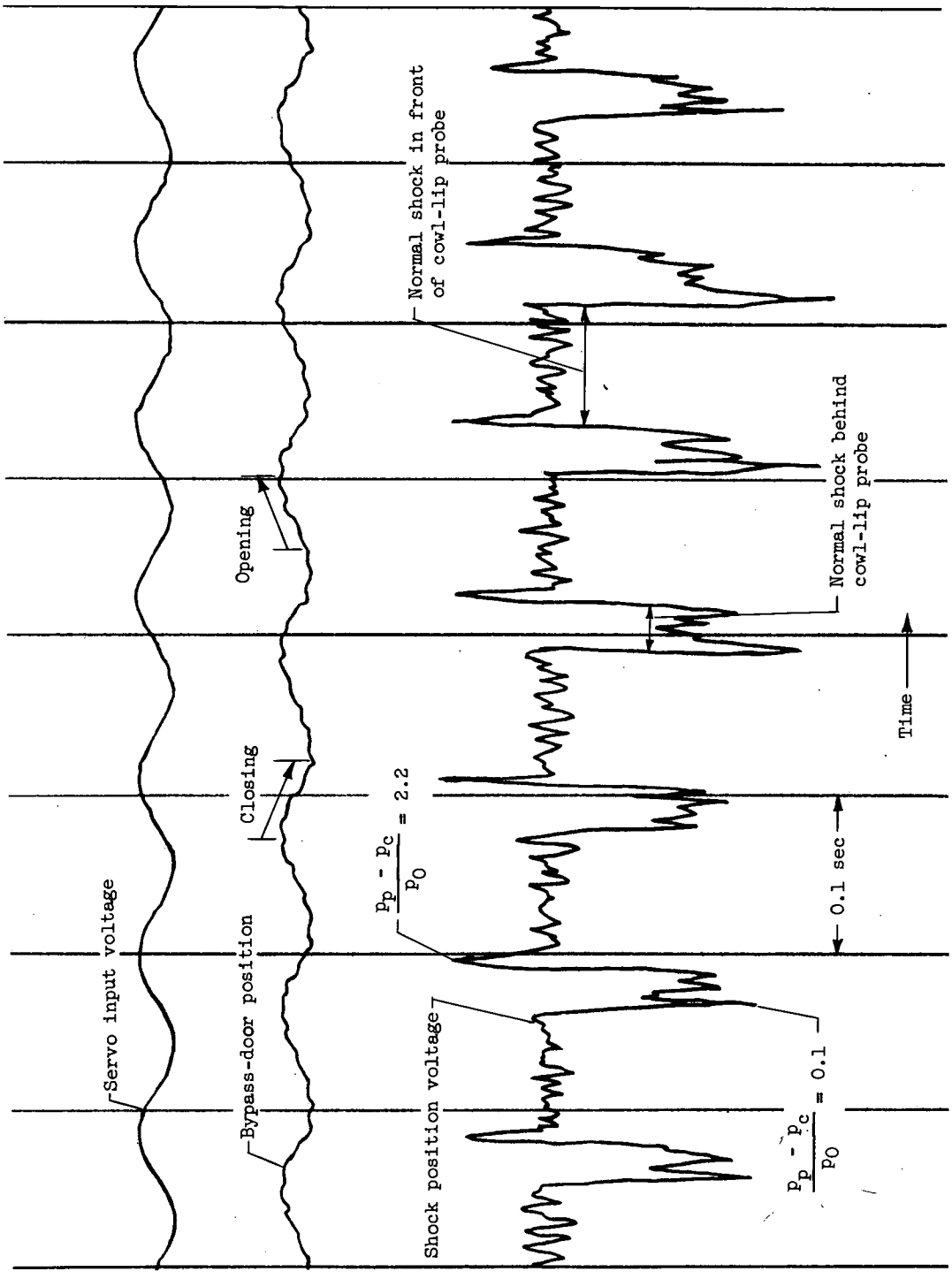

Figure 4. - Response of shock-sensing probe to bypass-door oscillation. Imposed frequency, 9 cycles per second; free-stream Mach number, 2.0.

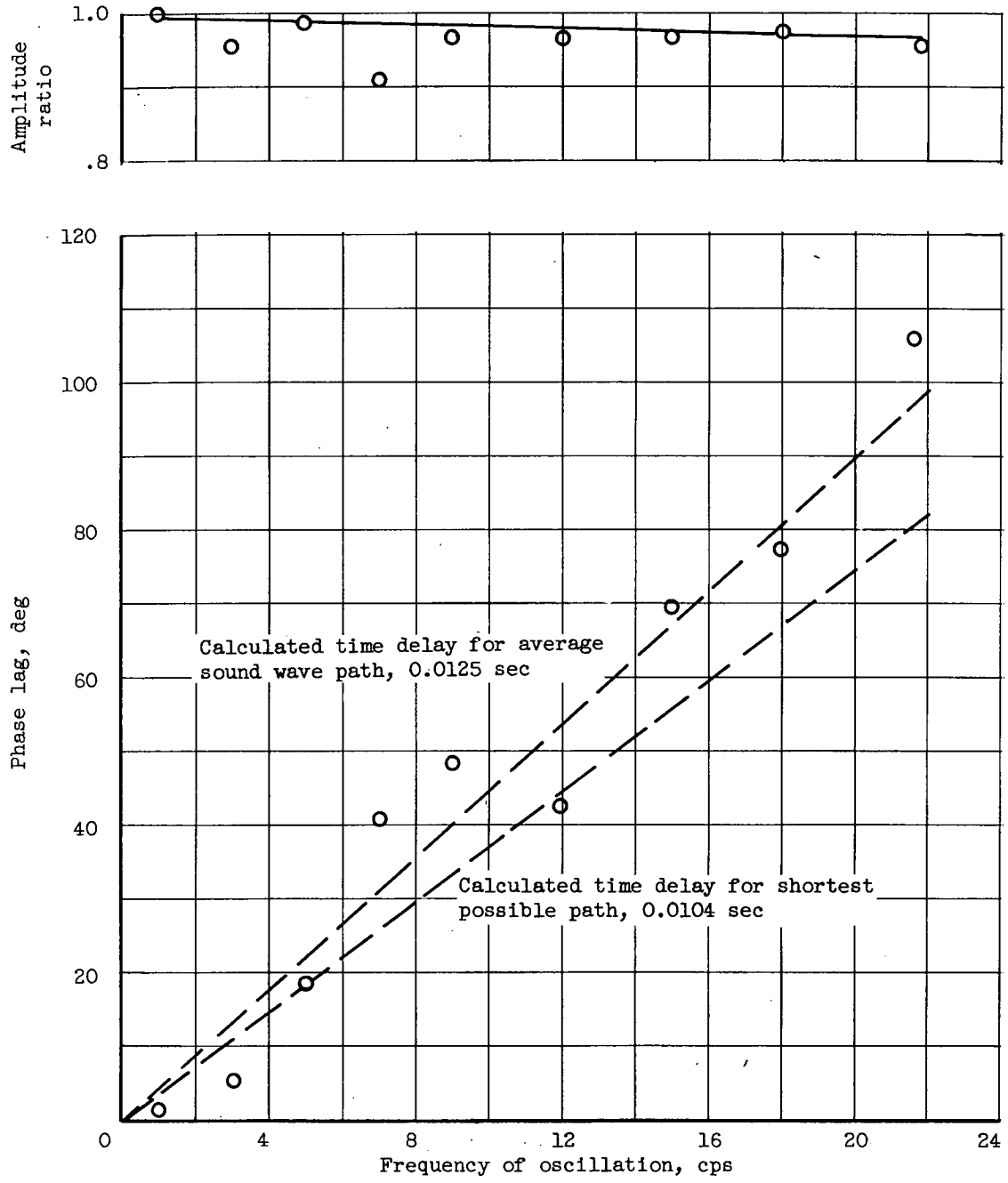

Figure 5. - Dynamic response of shock-sensing probe to bypass-door oscillation.

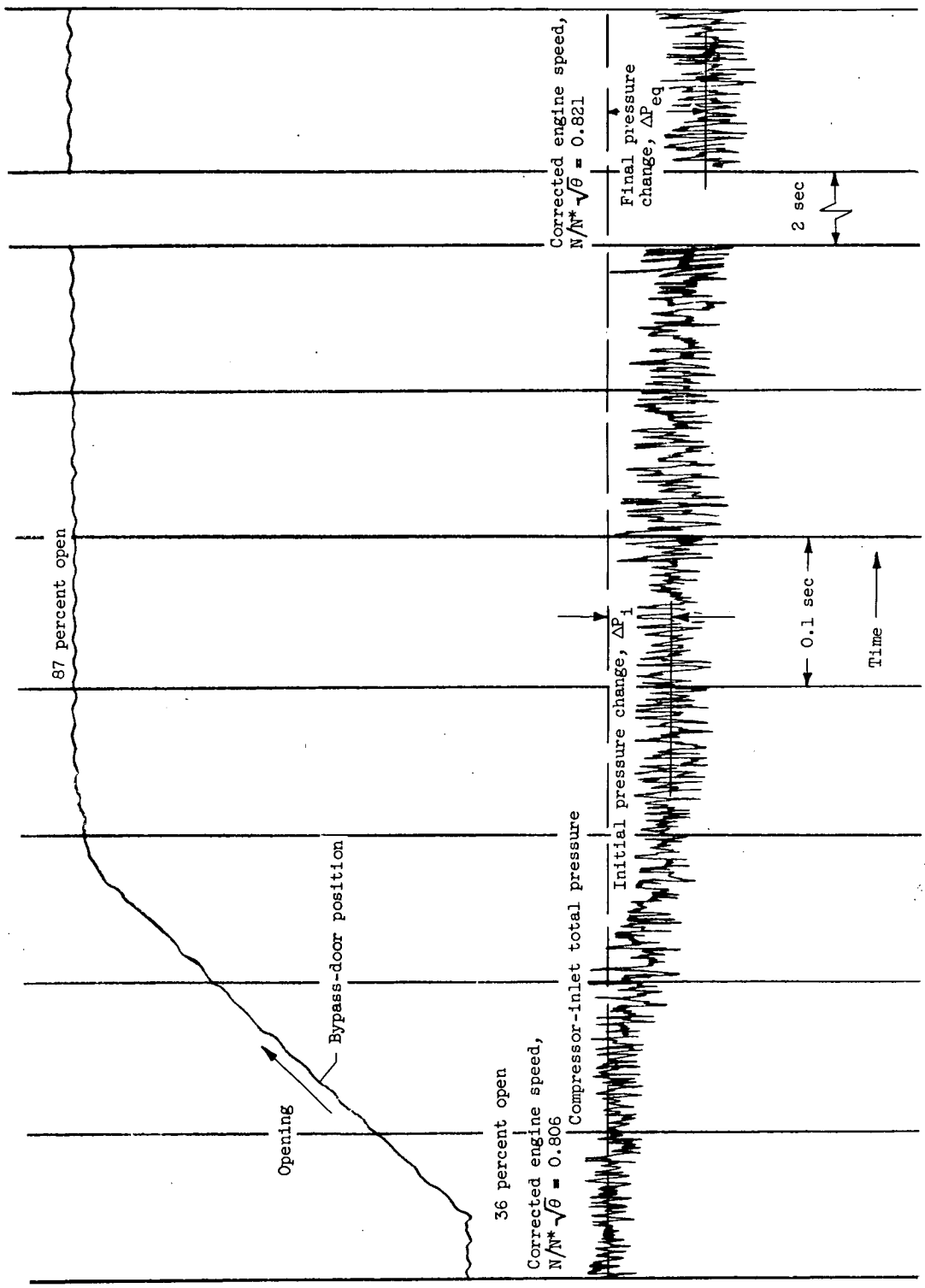

Figure 6. - Dynamic response of compressor-inlet pressure to bypass-door movement. (Run 5 of table I.) Inlet operation, supercritical; engine fuel flow, constant; free-stream Mach number, 2.0.

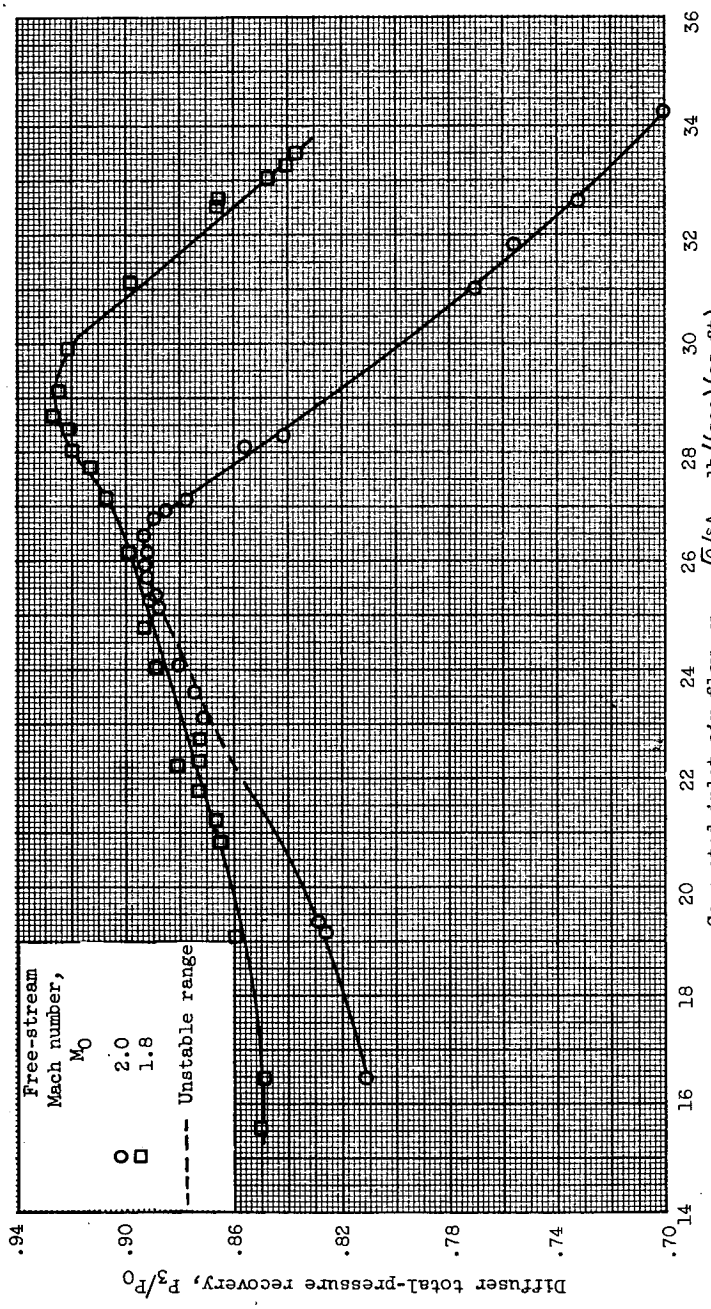

Figure 7. - Steady-state inlet performance.

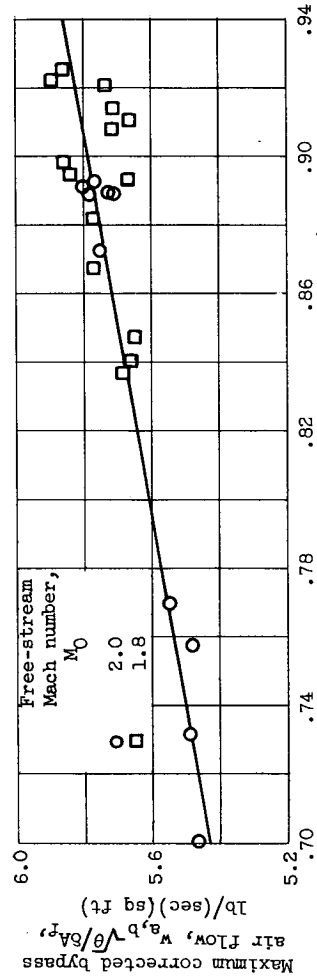

Figure 8. - Bypass air-flow characteristics.

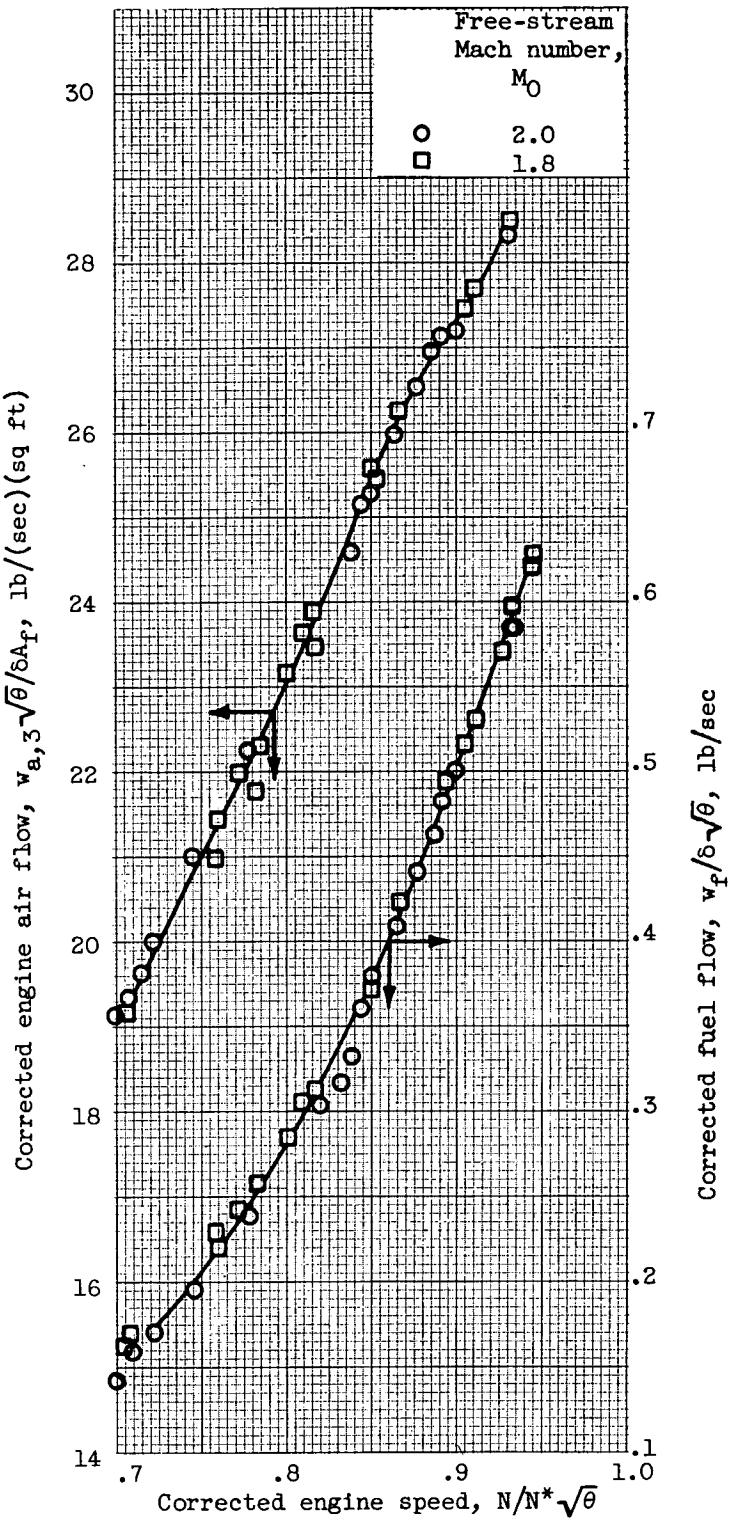

Figure 9. - Engine steady-state performance.